

Gastrointestinal Delivery of Glipizide from Carboxymethyl Locust Bean Gum- Al^{3+} -Alginate Hydrogel Network: *In Vitro* and *In Vivo* Performance

Paramita Dey,¹ Sabyasachi Maiti,² Biswanath Sa¹

¹Department of Pharmaceutical Technology, Jadavpur University, Kolkata 700032, West Bengal, India

²Department of Pharmaceutics, Gupta College of Technological Sciences, Ashram More, G. T. Road, Asansol 713301, West Bengal, India

Correspondence to: S. Maiti (E-mail: sabya245@rediffmail.com)

ABSTRACT: Sodium alginate and carboxymethyl locust bean gum (CMLBG) were reticulated in an aqueous solution of AlCl_3 , and this novel interpenetrating network (IPN) hydrogel encapsulated about 93–98% glipizide. The degree of reticulation in the spherical IPN beads was confirmed by Fourier transform infrared spectroscopy, elemental analysis, neutralization equivalent determination, tensile strength testing, and differential scanning calorimetry analysis. An increase in the CMLBG weight ratio and the degree of crosslinking in the IPN was found to increase mean dissolution time of the encapsulated drug. The dissolution efficiency was found to be much higher in the medium at pH 7.4 than at pH 1.2. The swelling of IPN depended on the pH of the medium, and accordingly, monitored the drug release for a period of 8 h. The anomalous drug transport mechanism was presumed to be operative. High performance liquid chromatography (HPLC) analysis showed the drug's stability in the IPN during encapsulation. The IPN showed significant hypoglycemic activity on male Wistar rats for up to 10 h. This could be beneficial for diabetic patients for achieving control over blood glucose levels. © 2012 Wiley Periodicals, Inc. *J. Appl. Polym. Sci.* 000: 000–000, 2012

KEYWORDS: hydrogels; interpenetrating networks (IPN); biopolymers; carboxymethyl locust bean gum; sodium alginate

Received 7 May 2012; accepted 29 June 2012; published online

DOI: 10.1002/app.38272

INTRODUCTION

Currently, natural polysaccharides, either in their native or tailored forms, have been investigated for the fabrication of drug-delivery devices, especially hydrogels. Hydrogels are macromolecular three-dimensional networks that imbibe water without being dissolved in water or biological fluids.^{1,2} In the swollen state, they become soft and rubbery and resemble living tissues, and they exhibit excellent biocompatibility.³

However, the major drawback of hydrogels is their poor mechanical properties, which are due to extensive swelling. Hence, their drug-release kinetics can be monitored by variation of the degree of crosslinking in the hydrogels; this regulates the propensity of fluid uptake.⁴ Numerous hydrogels have been described in the literature, and the attempts have included but have not been limited to the introduction of covalent crosslinks,⁵ grafting with polyacrylamide, poly(vinyl alcohol),^{6–8} and the use of polysaccharide blends.⁹ In contrast, interpenetrating polymer network (IPN) hydrogels have also gained considerable attention for controlled drug delivery.¹⁰ They are unique alloys

of crosslinked polymers in which at least one network has been synthesized and/or crosslinked in the presence of the other.^{11–13} They are often created for the purpose of conferring the key attributes of one of the components while maintaining the critical attributes of another. In some cases, entirely new properties that are not observed in either of the two single networks alone are exhibited by the IPNs.¹⁴ Interpenetration of the two networks may result in a higher mechanical strength than in the homopolymer network.¹⁵ Furthermore, IPNs provide free volume space for the easy encapsulation of drugs in their network structure.¹⁶

Sodium alginate (ALG) is an anionic, hydrophilic natural polysaccharide composed of D-mannuronic acid and L-guluronic acid residues.¹⁷ Its unique property of the formation of Ca^{2+} -alginate beads that enables the encapsulation of drugs.^{18,19} However, they exhibit poor mechanical stability in simulated intestinal fluid; this leads to the burst release of the loaded drugs.²⁰

Locust bean gum (LBG) is a nonionic, natural polysaccharide and consists of α -(1,4)-linked β -D mannopyranose backbone with branch points from their six positions linked to α -D-

galactose (1,6-linked α -D-galactopyranose).^{21–23} It is hardly soluble in water and needs heating to dissolve. To improve its water solubility and impart gelling ability, it requires chemical modification. Earlier, we reported that carboxymethyl locust bean gum (CMLBG) formed hydrogel beads with trivalent Al^{3+} ions, and the beads were able to control the drug release in phosphate buffer solution at pH 7.4.²⁴

This motivated us to develop IPNs of ALG with CMLBG to overcome the limitations of Ca^{2+} -ALG beads, especially in terms of their controlled release performance. IPN hydrogel beads of modified polysaccharides with native ones are limited in the literature, and notable examples include carboxymethyl xanthan/alginate.²⁵ Unfortunately, to date, there have been no reports on IPNs of CMLBG and ALG.

Glipizide is an oral hypoglycemic agent commonly used in type II diabetes mellitus. A short biological half-life of 3.4 ± 0.7 h demands its repetitive administration in 2–3 doses of 2.5–10 mg per day in the management of blood glucose level in adults.²⁶ Thus, glipizide was a suitable candidate for incorporation into a novel IPN of CMLBG and ALG. In this investigation, much emphasis was given to understanding the formulation variables that are likely to influence the properties and performance of this IPN.

EXPERIMENTAL

Materials

Glipizide was a gift sample from Micro Labs, Ltd. (Hyderabad, India). LBG was supplied by HiMedia Laboratories Pvt., Ltd. (Mumbai, India). ALG (molecular weight = 240 kDa) was procured from S. D Fine Chemical Pvt., Ltd. (Mumbai, India). Aluminum chloride (hexahydrate), monochloroacetic acid was obtained from Loba Chemie Pvt., Ltd. (Mumbai, India). Other reagents were of analytical grade and were used as received.

Synthesis of CMLBG

Carboxymethylation of polysaccharides is a well-known art.²⁷ The procedure adopted for LBG was same but with a little variation in that 4 mL of a 25% w/v LBG aqueous dispersion was preheated to 80°C for 15 min. To this, an aqueous solution of 55.89% w/v sodium hydroxide and 45.18% w/v monochloroacetic acid were added slowly at a milliliter ratio of 1.6 : 1 with the temperature of the mixture maintained at 15°C for 1.5 h. After that, the reaction was continued at 65°C for an additional hour, then cooled, washed with 80 : 20 (%v/v) methanol/water, and finally oven-dried at 40°C. The degree of *O*-carboxymethyl substitution in CMLBG was 0.56 ± 0.08 , and its aqueous solution (0.1% w/v) exhibited a viscosity 91.45 cP.

Fourier Transform Infrared (FTIR) Spectroscopy

KBr pellets of CMLBG, ALG, and drug-free CMLBG- Al^{3+} -ALG network were scanned in a PerkinElmer FTIR spectrometer (Spectrum RX1, PerkinElmer, Inc., Buckinghamshire, United Kingdom) from 4000 to 400 cm^{-1} , and the spectra were recorded.

Elemental Analysis

LBG and CMLBG (~ 2 mg) samples were analyzed for the percentage of carbon, hydrogen, and nitrogen by a CHNS/O elemental analyzer (2400 Series II, PerkinElmer, Inc., Waltham, Massachusetts, USA).

Properties of CMLBG, ALG, and Their Blends

Neutralization Equivalent (NE). NE is the equivalent weight of an acidic compound and was determined by titration with a standard base.²⁸ Five hundred milligrams of each homopolymer or their blend was dissolved in 150 mL of distilled water, and 40 mL of 0.1012M HCl was added to this. The solution was stirred continuously for 6 h and then back-titrated with a standard 0.1074M NaOH solution to neutralize the excess acid. A difference in the titer values of the blank and sample was considered the volume of NaOH required to neutralize the acid functional groups of the sample. This was done in triplicate, and the value of NE was estimated with eq. (1):

$$\text{NE(g)} = \frac{\text{Weight of the sample} \times 1000}{\text{mL of NaOH} \times \text{Normality}} \quad (1)$$

Determination of pH. The pH values of a 0.1% w/v CMLBG aqueous solution and those containing blends of ALG and CMLBG were determined by a pH meter (Thermo Scientific, Singapore).

Measurement of Viscosity. The aqueous solution viscosity (0.1% w/v) values of CMLBG and its blend with ALG was determined by a Brookfield viscometer (model A, Brookfield Engineering Labs., Inc., Middleboro, MA) at 32.7°C.

Tensile Strength. Drug-free IPN films were prepared by a solution casting method. The films were peeled off from the glass plate and crosslinked under conditions identical to those of the hydrogel preparation. Films $10 \times 100 \text{ mm}^2$ in size were fixed firmly to the upper and lower jaws of a universal testing machine (Hounsfield, model H25KS, Surrey, United Kingdom), and the tensile strength of the samples were measured at an extension speed of 20 mm/min.

Preparation of the CMLBG- Al^{3+} -ALG Hydrogel Network

Aqueous solutions were prepared at different weight percentage ratios of CMLBG-ALG for a total concentration of 4% w/v. The sol was loaded with 20% w/w drug and added dropwise through a 21G round flat-tipped needle into a 100 mL of a 5% w/v aqueous solution of aluminum chloride hexahydrate. The sol droplets were incubated in the gelation medium for 15 min, and hydrogel beads were produced. The beads were isolated by filtration, washed with distilled water ($3 \times 50 \text{ mL}$), and dried at 40°C. The details of the formulation variables are given in Table I. The drug-free or placebo hydrogel network beads were produced by the same method.

Scanning Electron Microscopy (SEM)

The gold-coated samples of the blank and drug-loaded IPN beads were photographed under a scanning electron microscope (JEOL JSM-6360, JEOL Ltd., Tokyo, Japan) at an acceleration voltage of 15 kV.

Measurement of the Bead Diameter

A digital caliper with an accuracy of 0.001 mm (model 99MAD014M, Tokyo) was used to measure the bead diameter. The diameters of 30 particles were measured for each formulation and averaged.

Table I. Composition of 4% (w/v) CMLBG–Al³⁺–ALG Hydrogel Network Beads

Formulation code	CMLBG–ALG (% w/w)	Strength of AlCl ₃ (% w/v)	Gelation time (min)	Drug load (% w/w of total polymer)
F1	25 : 75	5	15	20
F2	50 : 50	5	15	20
F3	75 : 25	5	15	20
F4	75 : 25	3	15	20
F5	75 : 25	1	15	20
F6	75 : 25	5	15	40
F7	75 : 25	5	15	60

Drug-Entrapment Efficiency (DEE)

Accurately weighed, 20 mg of beads was crushed with a mortar and pestle, and the drug was extracted overnight into 100 mL of a pH 7.4 phosphate buffer solution. The suspension was filtered, and the filtrate was assayed (UV1, Thermo Spectronic Ltd., Cambridge, United Kingdom) at a λ_{\max} of 276 nm. All samples were estimated four times. DEE of the hydrogel beads was calculated by eq. (2):

$$\text{DEE}(\%) = \frac{\text{Estimated drug content}}{\text{Theoretical drug content}} \times 100 \quad (2)$$

Swelling Behaviors

The blank beads (10 mg) were allowed to swell in 100 mL of simulated gastric solution (SGS; pH 1.2 KCl/HCl buffer without enzyme) and in simulated intestinal solution (SIS; pH 7.4 phosphate buffer without enzyme) separately, removed at certain intervals, blotted with tissue paper, and weighed (Precisa XB 600 MC, Precisa Instrument Ltd., Geneva, Switzerland). This process was continued for up to 2 h, and the swelling ratios were determined at each time point with eq. (3):

$$\text{Swelling ratio} = \frac{w_2 - w_1}{w_1} \quad (3)$$

where w_2 is the mass of swollen beads at time t and w_1 is the initial mass of dry beads. We studied the pulsatile swelling behavior of the beads by altering the pH of the surrounding medium (pHs of 1.2 and 7.4) at 37°C. The step changes followed an arbitrary sequence for a period of 8 h.

In Vitro Drug Release

The drug-release experiment was carried out in a paddle-type dissolution tester (VDA-6D, Veego Instruments Corp., Mumbai, India). For this, an accurately weighed 50 mg of beads was placed in 900 mL of SIS (pH 7.4), and the paddle was rotated at 50 rpm with the temperature maintained at $37 \pm 0.5^\circ\text{C}$. Five-milliliter aliquots were withdrawn at specified time intervals and were replenished immediately with the same volume of fresh medium. The samples were analyzed by a spectrophotometer (UV1, Thermo Spectronic) at 276 nm. This *in vitro* study was repeated in SGS (pH 1.2) for 2 h. Each study was con-

ducted four times, and the cumulative percentage of drug release was plotted as a function of time.

Differential Scanning Calorimetry (DSC)

The drug-free samples of CMLBG–Al³⁺–ALG hydrogel beads (~10–14 mg) were heated in a PerkinElmer Calorimeter (Pyris-Diamond Thermogravimetry/Differential Thermal Analyzer (TG/DTA), Singapore) at 15°C/min. The samples were heated in sealed aluminum pans under nitrogen purging at 20 mL/min. The thermal scanning was processed from 30 to 250°C.

Drug-Release Mechanism

The drug-release data were fitted to the simple power-law expression: $M_t/M_\infty = kt^n$, where M_t/M_∞ is the fraction of drug release at time t , k is the release rate constant, and n is the diffusion exponent that characterizes the drug-release mechanism.²⁹ A least squares regression method was used to determine the values of n and k . Values of $n = 0.43$ or less indicate Fickian transport, whereas values of n of 0.43–0.85 indicate anomalous or non-Fickian drug transport from spherical matrices.

Drug Stability in the Hydrogel Network

The formulations were stored in a programmable humidity test chamber (Remi Instruments Ltd., Mumbai, India) at 40°C/75% relative humidity for 3 months. The drug was extracted from fresh and aged samples into methanol, sonicated, and filtered through Whatmann filter paper with a pore size of 0.1 μm . The filtrate was further diluted with a solution of 0.05M potassium acid phosphate in methanol (40 : 60 v/v). The pH of the mobile phase was adjusted to 3.0 with phosphoric acid. Twenty microliters of both the standard (5 $\mu\text{g}/\text{mL}$) and test solutions were injected into an RP C18 column through a (7725i, Rheodyne LLC, Rohnert Park, Canada) injector. The mobile phase was set at a flow rate (isocratic) of 1.5 mL/min. High-performance liquid chromatograms were recorded at a UV detection wavelength of 230 nm. The retention time (RT) was observed, and the area under the peak was calculated. The absolute recovery was estimated by comparison of the peak area ratio of the samples to the standard glipizide according to eq. (4):

$$\text{Recovery}(\%) = \frac{\text{Area under the curve of the sample}}{\text{Area under the curve of the standard}} \times 100 \quad (4)$$

In Vivo Antidiabetic Activity

The *in vivo* blood glucose lowering activity of the hydrogel beads was studied on normal healthy male Wistar rats weighing 250–300 g each. The approval of the institutional animal ethics committee (955/A/06/CPCSEA) was obtained before the animal experiment. The animals were divided into two groups, each consisting of five animals. The animals were fasted (with water) at least 12 h before the study. On the day of experiment, normal blood glucose levels of the animals were measured. Experimental diabetes was induced by a single intraperitoneal injection of alloxan at 120 mg/kg body weight (BW) dissolved in normal saline. Rats were maintained on 5% glucose solution to prevent hypoglycemia for 5 days. Blood samples were taken from tail veins 5 days after the injection of alloxan to confirm the

induction of diabetes. Group I served as a control and received only distilled water. Group II received a glipizide-loaded bead formulation. The beads (800 $\mu\text{g}/\text{kg}$ BW) were administered orally with stomach intubation. Blood samples were collected at an hourly interval for a period of 12 h. The blood glucose levels were measured with Accu-Chek Sensor comfort test strips (Roche Diagnostics, Mannheim, Germany). The reduction in blood glucose level was measured and expressed as a percentage with time.

Statistical Analysis

The effects of the formulation variables on the DEE and release rate were tested for significance with one-way analysis of variance: single factor in Microsoft Excel. A significant difference was indicated at $p < 0.05$. The data were averaged and represented by standard deviation (SD). The standard error of the mean and the coefficient of variation were also calculated to represent and explain the data.

RESULTS AND DISCUSSION

IPN Hydrogel Structure and Bead Properties

Ionotropic gelation of the CMLBG–ALG blends with aluminum (Al^{3+}) ions led to the formation of the IPN hydrogel structure. The formation of a reticulated structure was examined by FTIR spectroscopy. In the spectrum of ALG [Figure 1(a)], the asymmetric and symmetric stretching vibration of the carboxylate anions was noted at wave numbers of 1610.27 and 1415.49 cm^{-1} , respectively. A wide band of $-\text{OH}$ stretching vibrations appeared at 3442.31 cm^{-1} . A similar spectrum was reported for ALG.³⁰ The bands of asymmetric and symmetric $\text{C}=\text{O}$ stretching in COO^- ions were noted at 1594.84 and 1415.49 cm^{-1} , respectively, in the spectrum of CMLBG [Figure 1(b)]. A broad band at 3474.13 cm^{-1} corresponded to the hydroxyl ($-\text{OH}$) stretching vibrations. However, an additional peak associated with the carbonyl ($\text{C}=\text{O}$) stretching of carboxymethyl groups was traced at 1328.71 cm^{-1} , although it was not evident in the IR spectrum of LBG. Identical bands were found in carboxymethylated starch³¹ and cellulose.³² Elemental analysis further supported the carboxymethylation of native LBG. In the sample of LBG, the carbon and hydrogen contents were found to be 29.19 and 5.57%, respectively, but the same was higher for the CMLBG sample, that is, 38.50 and 9.27%, respectively.

Because of the overlapping of the $-\text{OH}$ functional groups of the polymers, the $-\text{OH}$ stretching vibration broadened at 3410.49 cm^{-1} in IR spectrum of the drug-free beads [Figure 1(c)]. However, the asymmetric (1634.38 cm^{-1}) and symmetric (1477.21 cm^{-1}) carboxyl stretching of CMLBG and ALG shifted to higher wave numbers in the drug-free IPN beads. Thus, it became explicit that there was an ionic interaction between the negatively charged COO^- groups of the polymers and oppositely charged Al^{3+} ions. The polysaccharides had backbone chains composed of β -glycosidic linkages, and this was characterized by the bands that appeared in the range of 870–900 cm^{-1} in their individual and combined spectra. Thus, it was ascertained that the ionically crosslinked IPN network of CMLBG and ALG was produced.

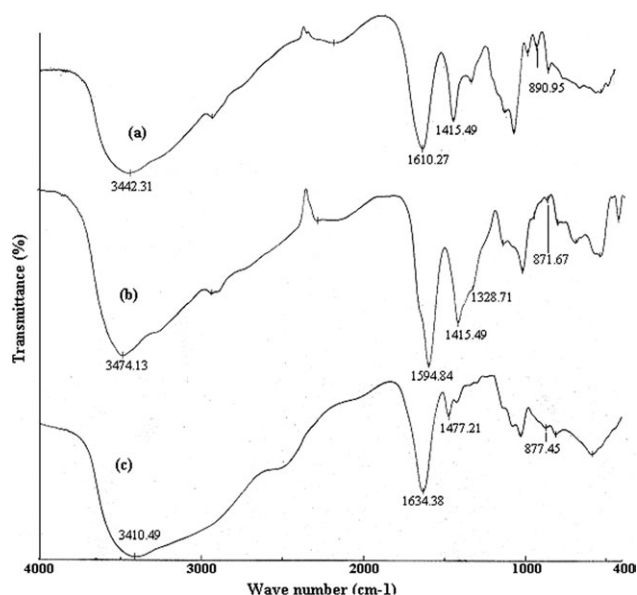


Figure 1. FTIR spectra of (a) ALG, (b) CMLBG, and (c) drug-free IPN hydrogel.

IPN hydrogel beads were prepared at various compositions of drug loading, homopolymer ratio, and crosslinker concentration (Table I). SEM photographs of the drug-free and drug-loaded beads are displayed in Figure 2(a–d). Regardless of the variables, the beads were spherical in both the wet and dry states. When examined under SEM at 35 and 50 \times magnifications, no microscopic cracks were visible over their surface. This was contrary to an earlier finding of Ray et al.²⁵ They showed that IPN beads of carboxymethyl xanthan and ALG were distorted after drying, and their surface became rough and folded. However, the effect of the formulation variables was evident on the bead diameter (Table II). For a total polymer concentration of 4% w/v, increases in the weight percentage of CMLBG of 25, 50, and 75% w/w systematically decreased the bead diameter from 1245 to 1079 μm with coefficients of variation of 0.25 and 0.35%, respectively (Table II). It was reported that an increase in the weight ratio of the graft copolymer (1.5 : 1.5 to 2 : 1) increased the size of the poly(acrylamide-*g*-xanthan)–carboxymethylcellulose IPN beads from 944 to 1048 μm .⁶ They reasoned the formation of bigger droplets during the extrusion of a highly viscous solution at the higher copolymer concentration. In our case, as shown in Table III, the variation in the polymer ratio did not cause any appreciable change in the solution viscosity (94.36–98.25 cP). Hence, the effect of the CMLBG–ALG ratio on the bead size could not be explained by the solution viscosity but rather was possible by the determination of NE. The NE value indicates the number of carboxyl groups (basicity) of polybasic acid and is determined by neutralization with a standard sodium hydroxide solution. The greater number of carboxyl groups in a sample indicates the lower NE value. The values of NE followed the descending order 2026, 1926, and 1726 g, respectively, with increasing percentage of CMLBG in the blend (Table II). It was conspicuous that a higher number of carboxyl groups promoted stronger interaction with Al^{3+} ions and

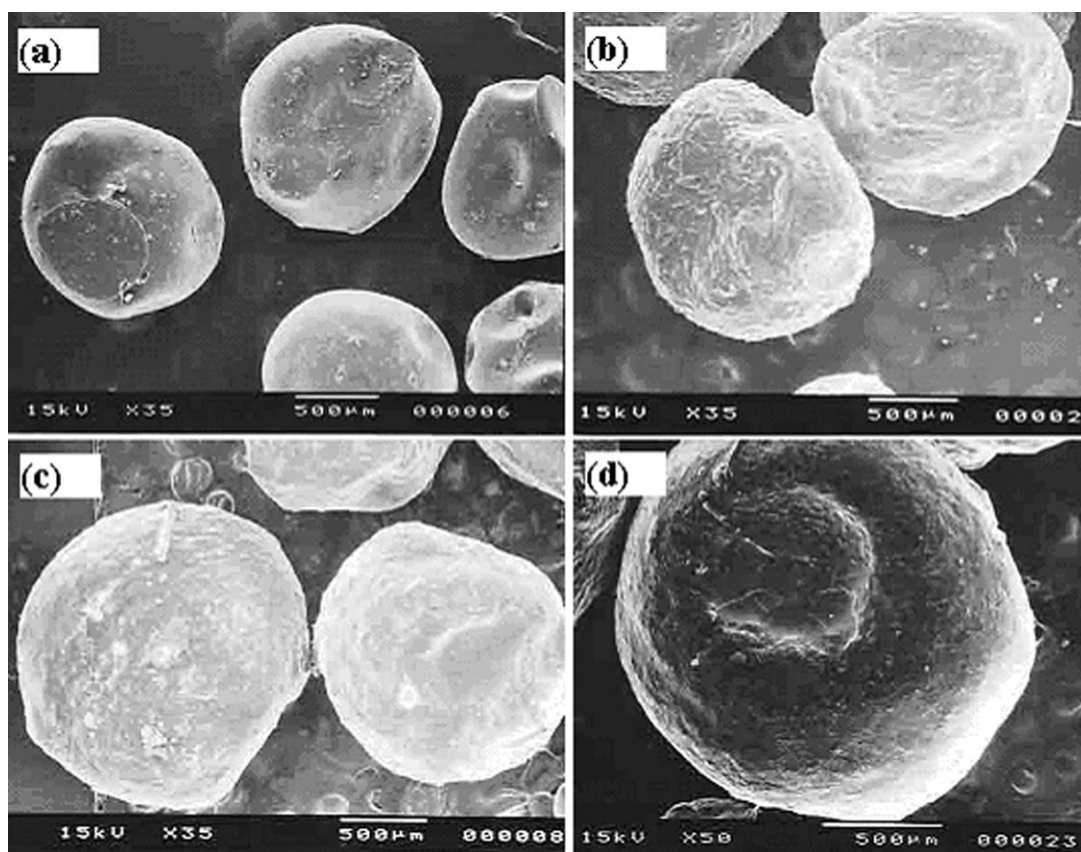


Figure 2. SEM photographs of the CMLBG–ALG (3 : 1) hydrogel beads: (a) blank bead with 5% AlCl₃, (b) bead with a 20% drug load and 5% AlCl₃, (c) bead with a 20% drug load and 1% AlCl₃, and (d) bead with a 60% drug load and 5% AlCl₃.

caused more shrinkage of the beads at higher percentage of CMLBG and finally reduced the bead size. This was further appreciated by the values obtained after measurement of the tensile strength of the IPN films. With the incorporation of a larger proportion of CMLBG in the blend, a higher mechanical strength was attained, and it was about 1.31 times higher for the IPN having a CMLBG–ALG weight percentage ratio of 75 : 25 (Table II). This was attributed to strong reticulations with the metal ions and the interpenetrations of a large number of polymer chains in the IPN beads.³³

Smaller IPN beads were also produced when the metal salt (AlCl₃) concentration was increased from 1 to 5% w/v. DSC traces of the drug-free IPN beads are presented in Figure 3. The melting endothermic transition of the beads prepared with the lowest metal ion strength was noted at 166.10°C with an enthalpy of 126.2810 J/g [Figure 3(a)]. At the intermediate AlCl₃

strength, a total enthalpy (ΔH) of 658.3112 J/g was calculated for the endothermic transitions at 140.95 and 182.13°C [Figure 3(b)]. With a further increase in the crosslinker concentration, a comparatively higher ΔH value (757.8794 J/g) was found for the thermal peaks of 143.98 and 183.02°C [Figure 3(c)]. Higher ΔH values indicated higher crosslinking in the beads. During incubation, the beads shrank and formed smaller beads at higher concentrations of AlCl₃. Conversely, the higher drug loadings up to 60% w/w generated larger particles. This might have been due to the fact that the drug occupied the interstitial spaces between the polymer segments.³⁴

Likewise, the DEE of the IPN beads was also influenced by the formulation variables. The aqueous polymer blends of CMLBG–ALG exhibited a value around pH 10 (Table II). Glipizide is a weak acid with pK_a of 5.9. It is insoluble in water, but a higher solubility was expected at pH values above its pK_a . At alkaline

Table II. Physicochemical and Mechanical Properties of the CMLBG and ALG Blends

CMLBG–ALG (% w/w)	NE (g) ± SD (n = 3)	pH of the aqueous solution	Viscosity (cP) ± SD (n = 3)	Tensile strength (MPa) ± SD (n = 3)
25 : 75	2026 ± 1.52	10.32	94.36 ± 1.32	50.12 ± 0.12
50 : 50	1926 ± 1.43	10.22	95.45 ± 1.52	58.75 ± 0.97
75 : 25	1726 ± 1.45	10.13	98.25 ± 1.42	65.78 ± 0.75

Table III. Effect of the Formulation Variables on the Properties of the CMLBG–Al³⁺–ALG Hydrogel Beads

Formulation code	Bead diameter (μm) ± SD	Entrapment efficiency (% ± SD, n = 4)	pH 7.4 buffer solution (Mean ± SD, n = 4)		DE (%) ± SD (n = 4)	
			t _{50%} (h)	MDT _{50%} (h)	In acid	In alkali
F1	1245 ± 3.12	93.93 ± 0.65	2.68 ± 0.09	1.08 ± 0.05	11.40 ± 1.12	56.39 ± 0.83
F2	1135 ± 6.12	94.55 ± 0.39	3.40 ± 0.11	1.40 ± 0.03	9.49 ± 0.50	49.88 ± 0.63
F3	1079 ± 4.26	96.91 ± 0.71	4.13 ± 0.15	1.83 ± 0.09	6.74 ± 0.13	41.76 ± 0.82
F4	1205 ± 4.85	94.07 ± 0.56	3.63 ± 0.15	1.57 ± 0.06	15.94 ± 0.73	49.26 ± 0.52
F5	1258 ± 5.12	93.13 ± 0.31	3.25 ± 0.24	1.29 ± 0.05	21.17 ± 0.45	53.32 ± 0.55
F6	1138 ± 3.75	97.85 ± 0.61	2.93 ± 0.10	1.15 ± 0.01	20.25 ± 0.16	54.25 ± 0.09
F7	1272 ± 8.45	98.42 ± 0.74	2.08 ± 0.09	0.79 ± 0.01	24.64 ± 0.03	63.02 ± 0.13

pH in the gum solutions, the drug dissolved to a lesser extent, and that fraction diffused out of the hydrogel matrix in the gelation medium during the crosslinking reaction. Hence, there was little chance of achieving 100% DEE in the IPN beads. It is noteworthy to mention that DEE also depended on the amount of crosslinker and the degree of crosslinking in the IPN. In accordance with our earlier discussion with the effect of CMLBG–ALG weight percentage ratio on the degree of crosslinking, the IPN showed the lowest entrapment efficiency (93.93%) at 25% CMLBG, and the highest (96.91%) was at 75% CMLBG, with coefficients of variation of less than 1%. The mean DEE values assumed a statistically significant difference ($p < 0.05$).

The DEE of the IPN decreased at a low concentration of AlCl₃, and a reduction of 3.90% was incurred when the amount of crosslinker was set at 1%. The statistical difference in the mean DEE of the IPNs was evident ($p < 0.05$). At low strength, the network might be loose and ensured faster drug diffusion through the large pores/channels into the external gelation medium. Ray et al.²⁵ stated that the concentration of metal ions did not cause any appreciable change in the DEE of the IPN beads of sodium carboxymethyl xanthan gum and ALG (1 : 1). However, the DEE of the IPN was found to decrease from 97.65 to 97.22% with decreasing concentration of AlCl₃ (from 8 to 2% w/v) when it was prepared at a total polymer concentration of 3% w/v.

As can be seen from Table III, there was a marginal difference between the DEE values of the IPN beads having an unequal drug loading ($p < 0.05$). A recent literature report on an IPN of poly(*N*-isopropyl acrylamide)–gellan gum (70 : 30, %w/w) indicated that the encapsulation efficiency (56 to 64%)

improved at drug loadings of 25–50% w/w, respectively.³⁵ Kumbar et al.³⁶ also demonstrated that the encapsulation efficiency of polyacrylamide-*g*-guar gum and ALG network beads increased from 61.31 to 65.51%, respectively, at 10 and 20% w/w extremes of chlorpyrifos loading.

Swelling versus Drug Release

Figures 4(A), 5(A), and 6 illustrate the cumulative percentage drug release versus time profiles of the IPN beads. After oral administration, the drug is usually absorbed from the variable pH environment of the gastrointestinal (GI) tract. As the pH of the GI tract varies from acidic to weakly alkaline, the drug-release behaviors of the IPN beads were demonstrated in both SGS (pH 1.2) and SIS (pH 7.4).

To characterize the drug-release process, the dissolution efficiency (DE; %) of the IPN was calculated by the following model equation:³⁷

$$DE(\%) = \frac{\int_0^t y dt}{y_{100} t} \times 100 \quad (5)$$

where y is the drug percentage dissolved at time t and y_{100} is the 100% drug dissolution at time t . For a definite period of 2 h, we calculated the DE of the IPN by measurement of the area under the percentage drug release versus time curve by (NCSS 8 Free Trial, NCSS Statistical Software, Kaysville, Utah, USA) and then putting values into eq. (5).

As the weight fraction of CMLBG in the IPNs was increased to 75%, the DE values reduced from 11.40 to 6.74% in SGS. Such a tendency adhered to SIS but with relatively higher values (Table III). In media like this, DE decreased systematically with higher AlCl₃ strength (Table III). Keeping all of the variables constant, an increase in the initial drug loading accelerated the drug-release rate (Table III) and resulted in a higher DE. This could have been due to the modulation of drug diffusion from the IPN with increasing drug load. Of all the formulations, DE was found to be higher at a loading of 60% and had a proportional relation with the initial drug loading (Table III). It became easier to understand that the proportion of polymer per unit weight decreased and thus weakened the IPN hydrogel network at higher loads. Because of the higher concentration gradient, the rate of molecular diffusion may have been much greater

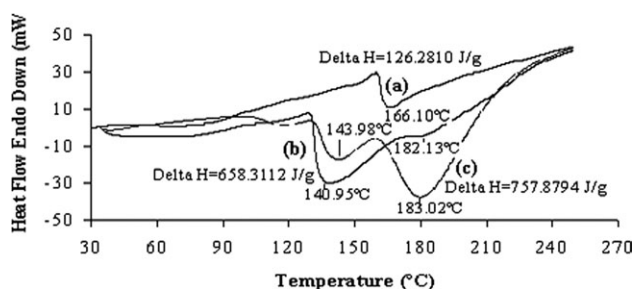


Figure 3. DSC thermograms of the drug-free CMLBG–Al³⁺–ALG hydrogel beads. Strength of AlCl₃ (% w/v): (a) 1, (b) 3, and (c) 5%.

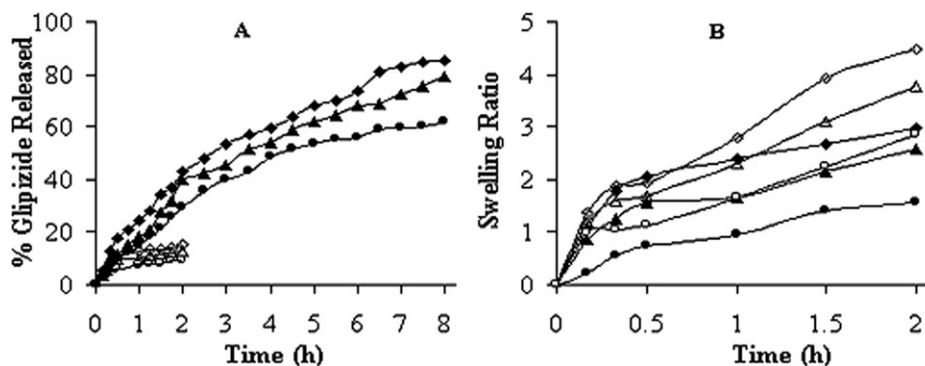


Figure 4. (A) Release profiles of CMLBG–Al³⁺–ALG hydrogel beads in SGS (open symbols) and SIS (closed symbols). CMLBG–ALG = (Δ) 1 : 1, (\diamond) 1 : 3, and (\square) 3 : 1. Maximum standard error of the mean = 1.35 ($n = 4$). (B) Swelling ratios of the drug-free CMLBG–Al³⁺–ALG hydrogel beads in SGS (open symbols) and SIS (closed symbols). CMLBG–ALG: (Δ) 1 : 1, (\diamond) 1 : 3, and (\square) 3 : 1. Maximum standard error of the mean = 0.10 ($n = 3$).

and, consequently, assured a higher drug-release rate in the dissolution medium.³⁸

The dissolution parameters, including the mean dissolution time (MDT_{50%}) and the time to release 50% of drug ($t_{50\%}$), were used to compare the dissolution data of the formulations in SIS. MDT reflects the time for the drug to dissolve and is the first statistical moment for the cumulative dissolution process and provides an accurate drug-release rate. A higher MDT value indicates a greater drug-release-retarding ability.³⁹ MDT_{50%} was calculated according to eq. (6):

$$MDT_{50\%} = \frac{\sum_{i=1}^{i=n} t_{mid} \times \Delta M}{\sum_{i=1}^{i=n} \Delta M} \quad (6)$$

where i is the dissolution sample number, n is the number of time increments considered, t_{mid} is the time at midpoint between t_i and t_{i-1} , and ΔM is the additional amount of drug dissolved between time t_i and t_{i-1} .⁴⁰

As the proportion of CMLBG increased, the release rate decreased, as evident by the MDT_{50%} and $t_{50\%}$ values. The trend remained unaltered as the crosslinker concentration was increased for the beads (Table III). However, on the basis of their MDT_{50%} and $t_{50\%}$ values, a faster drug-release rate was assumed for the beads at higher loadings. Considering each variable, we analyzed statistically that the MDT_{50%} and $t_{50\%}$ val-

ues of the formulations fluctuated significantly ($p < 0.05$). Furthermore, a maximum of about 89% drug release was approximated at the 8th h in SIS. This signified that the IPNs did not liberate their 100% content, and they needed more time to complete drug release in SIS.

However, it was understood that the drug-release rate from the IPNs was comparatively slower in SGS. The saturation solubility of glipizide in the KCl/HCl buffer (pH 2.0) solution was reported to be 1.1 $\mu\text{g/mL}$,⁴¹ and hence, the slower release of glipizide from the IPNs could be expected in SGS. In addition, the beads swelled and deswelled, depending on pH of the swelling medium and, therefore, could influence the drug-release rate. To substantiate this, the swelling behavior of the drug-free beads was examined in SGS at pH 1.2 and in SIS at pH 7.4.

The swelling ratio versus time curves of the drug-free IPN beads are shown in Figures 4(B) and 5(B). As was evident from the figures, the swelling ratio of the beads in SIS was much greater than that observed in SGS at higher concentrations of CMLBG and AlCl₃. With increasing ratios of CMLBG (25, 50, and 75%) in the IPN, the swelling ratios increased by 49.83, 46.42, and 60.67%, respectively, in SIS versus SGS at the end of 2 h. The swelling ratios of the IPN beads were higher in SIS than in SGS at each time point for particular metal-ion concentrations. In other words, the swelling ratio of the IPN decreased with increasing concentration of metal ions (1–5% w/v) and

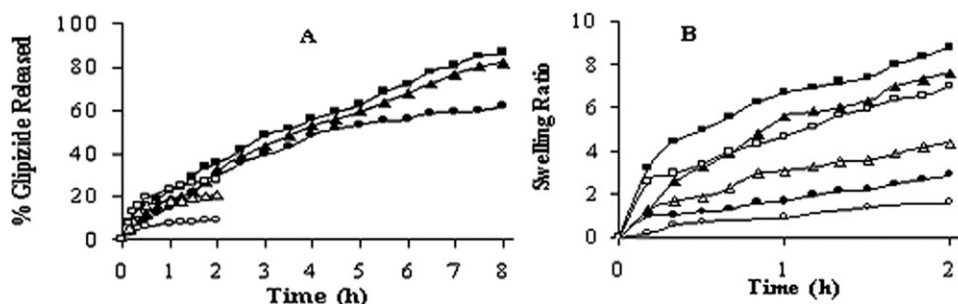


Figure 5. (A) Release profiles of CMLBG–Al³⁺–ALG hydrogel beads in SGS (open symbols) and SIS (closed symbols). Strength of AlCl₃: (\square) 1, (Δ) 3, and (\square) 5%. Maximum standard error of the mean = 1.42 ($n = 4$). (B) Swelling ratios of drug-free CMLBG–Al³⁺–ALG hydrogel beads in SGS (open symbols) and SIS (closed symbols). Strength of AlCl₃ = (\square) 1, (Δ) 3, and (\square) 5%. Maximum standard error of the mean = 0.04 ($n = 3$).

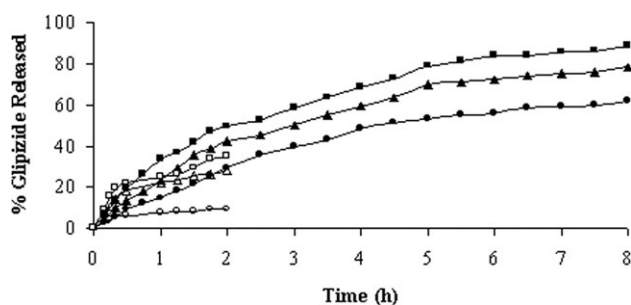


Figure 6. Release profiles of the CMLBG- Al^{3+} -ALG hydrogel beads in SGS (open symbols) and SIS (closed symbols). Drug loading = (\square) 20, (\triangle) 40, and (\circ) 60%. Maximum standard error of the mean = 1.53 ($n = 4$).

corresponded to 25.75, 74.83, and 60.67% higher values in SIS, respectively, at the end of the swelling study.

The carboxyl groups of the IPN remained in ionized form in SIS (pH 7.4), which would break hydrogen bonds and generate electrostatic repulsion among the polymer chains. The repulsive-force-initiated expansion of the network attracted more water into the hydrogel network and caused higher swelling in the hydrogel beads. On the other hand, the carboxyl groups were protonated in SGS (pH 1.2) and formed much more hydrogen bonds with the hydroxyl groups; this led to a compact hydrogel network structure that restricted the movement and relaxation of the network chains.⁴² Thus, rapid swelling of the IPN could be expected in SIS versus SGS and accounted for the higher drug-release rate in SIS.

It is well known that the drug release from calcium-ALG beads is minimal in acidic media,⁴³ but the same release is much faster in phosphate buffer solution above pH 5.5 because of the rapid disruption of the gel matrix.⁴⁴ It has been reported that ALG undergoes proton-catalyzed hydrolysis and is dependent on the pH.⁴⁵ The calcium-ALG bead system alone, therefore, can undergo a reduction in the alginate molecular weight; this results in faster disintegration and the release of a molecule when the gel is reequilibrated in a neutral pH solution.⁴⁶ Therefore, it would be very interesting if a study was designed to understand the swelling and deswelling tendency of drug-free

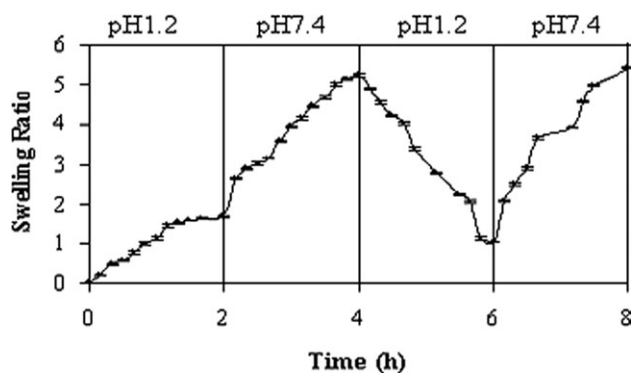


Figure 7. Pulsatile swelling behaviors of the drug-free CMLBG- Al^{3+} -ALG hydrogel beads (F3).

IPN beads in a pulsatile pH environment. This property was illustrated for one of the IPN formulations (F3), and Figure 7 depicts the real picture. After swelling in SGS (pH 1.2) for 2 h, the IPN beads were exposed to SIS (pH 7.4), and the swelling ratio increased by 44.55% in 0.5 h with a final rise of 212.50% at the 4th h. Thereafter, the beads deswelled in SGS by 80% at the 6th h; however, the ratio suddenly rose to 416.19% in SIS at the end of 8 h. The deswelling process can be interpreted as follows. When the beads were put into SGS, the hydrogen ions (H^+) diffused into the swollen beads, simultaneously exchanged with surface Na^+ ions, and formed a neutral layer of deswelled polymer around the core; this still remained in Na^+ form and, therefore, in the swollen state. When the beads were exposed to SIS, the shell of nonionic carboxyl groups (RCOOH) converted to Na^+ form (RCOO^-Na^+), and the swelling process restarted.⁴⁷ The drug-free IPN beads did not disintegrate in SIS when they were transferred immediately after 2 h of incubation in SGS and, thus, exhibited their potential in dictating drug release according to the variable pH region of the GI tract.

During data analysis, it was revealed that the swelling depended on the ratio of CMLBG and, consequently, the degree of crosslinking in the IPN beads. An increase in the CMLBG ratio and AlCl_3 concentration led to more crosslinked IPN structures, and accordingly, the beads deswelled. At a low crosslinking density, the hydrogel network became loose with a greater

Table IV. Effect of the Formulation Variables on the Drug-Release Mechanism from the CMLBG- Al^{3+} -ALG Hydrogel Beads

Formulation code	Korsmeyer–Peppas model					
	pH 1.2 KCl/HCl buffer solution			pH 7.4 phosphate buffer solution		
	k	n	r^{2a}	k	n	r^2
F1	0.1189	0.4957	0.8853	0.2467	0.6949	0.9833
F2	0.0998	0.4368	0.9076	0.1979	0.7569	0.9888
F3	0.0719	0.4416	0.9157	0.1450	0.8143	0.9793
F4	0.1674	0.4664	0.8448	0.1872	0.7383	0.9946
F5	0.2233	0.4527	0.9038	0.2364	0.6047	0.9944
F6	0.2175	0.4646	0.9615	0.2241	0.8061	0.9842
F7	0.2606	0.4303	0.9046	0.2979	0.7121	0.9793

^a r^2 , correlation coefficient.

hydrodynamic free volume, absorbed more of the liquid medium, and ensured higher swelling of the beads. To put it another way, an increase in the CMLBG ratio actually reduced the amount of ALG in the IPN beads. ALG suffers from a loose network structure. Thus, the bead pore size decreased with a subsequent reduction of the ALG proportion, made the solvent penetration difficult, and finally resulted in a lesser degree of swelling.⁴⁸ Therefore, the degree of crosslinking and consequent swelling would be responsible for the variable drug-release rate from different IPN bead formulations.

To gain an understanding of the drug-release mechanism from a hydrophilic glassy matrix, the release data were molded into a Korsmeyer–Peppas equation. Regardless of the formulation variables, the values of n ranged from 0.4303 to 0.4957 in SGS and from 0.6047 to 0.8143 in SIS (Table IV). Therefore, it became explicit that the drug release deviated from Fickian behavior and followed an anomalous diffusion mechanism. That is, the drug release was modulated by a combination of simple diffusion and polymer relaxation. In situations where the conventional sorption of a penetrate led to significant swelling and dimensional changes in the polymer matrix, the conventional Fick's law of diffusion did not apply as such.⁴⁹ The homogeneous glassy matrix imbibed water, and the polymer swelled to form a rubbery gel-like layer initially on the surface and then pervaded the entire matrix until the gel reached equilibrium. The dissolved drug diffused through the rubbery region to the external release medium. In addition to this drug-release path-

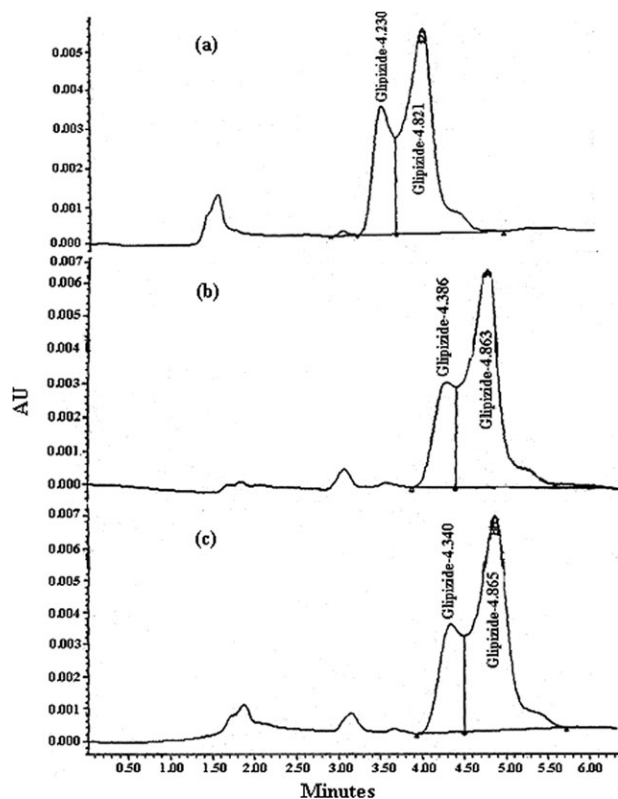


Figure 8. HPLC chromatograms of the (a) standard drug and the drug extracted from (b) fresh and (c) aged beads. [AU = Area Units].

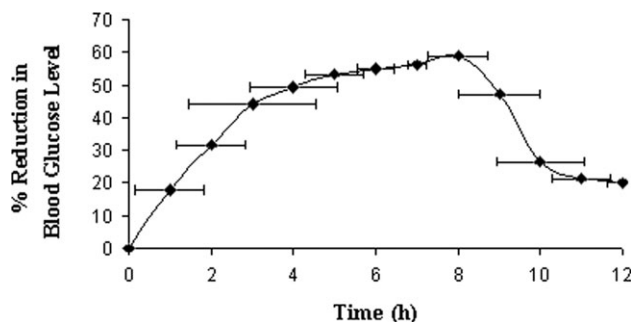


Figure 9. *In vivo* hypoglycemic activity of the CMLBG–Al³⁺–ALG hydrogel beads in male Wister rats.

way, the matrix erosion after polymer relaxation also contributed to the overall drug release.

Stability and *In Vivo* Antidiabetic Activity

High performance liquid chromatography chromatograms of standard glipizide were observed at RTs of 4.230 and 4.821 min and were totaled for the area under the curve to be 221,296 [Figure 8(A)]. The drug extracted from fresh IPN beads showed chromatograms at RTs of 4.386 and 4.863 min, and an area of 241,099 was computed [Figure 8(B)]. For the drug extracted from an aged sample, the RTs (4.340 and 4.865 min) were in close proximity to that observed in a fresh sample and covered an area under the curve of 242,010 [Figure 8(C)]. The percentage recovery was more than 100%, and the percentages were found to be 108.95 and 109.36% for fresh and aged samples, respectively. This suggested that the drug was stable in the IPN beads.

Considering all of the formulations, we observed that the IPN beads bearing the formulation code F3 ensured a reasonable DEE and provided the slowest drug-release profile. Hence, the formulation F3 was selected and tested for its prolonged hypoglycemic potentials. The *in vivo* hypoglycemic activity of the IPN was evaluated in male Wistar rats. The percentage reduction in the blood glucose level versus time curve is depicted in Figure 9. A maximum reduction of $58.96 \pm 0.72\%$ in the blood glucose level was observed at the 8th h after oral administration of the IPN beads. Kahn and Shechter⁵⁰ suggested that a 25% drop in the blood glucose level could be considered as a significant hypoglycemic effect. The hypoglycemic activity was significant between the 2nd ($31.59 \pm 0.85\%$) and 10th h ($26.83 \pm 1.07\%$). Under *in vivo* situations, the dosage form normally passes through the stomach (acidic) and then drained into the intestinal region (weakly alkaline). During its passage, the drug was released slowly, and consequently, it was absorbed through the GI mucosa. This further suggested that the IPN beads did not disintegrate in SIS, liberated the drug slowly, and showed a prolonged hypoglycemic effect. After that, the blood glucose level of the rats recovered to their normal levels.

CONCLUSIONS

In this study, an interpenetrating hydrogel network of CMLBG–Al³⁺–ALG was formulated for a model hypoglycemic agent, glipizide, and its performance was evaluated both *in vitro* and

in vivo. SEM revealed the spherical shape of the bead particles. Depending on the formulation variables, a DEE of as high as 98.42% was achieved. Within a timeframe of 2 h, the efficiency of drug dissolution from the IPNs was comparatively less in SGS. IPNs were able to prolong the drug release beyond 8 h. The swelling of the beads was responsible for the variable drug-release rate of the IPNs. HPLC analysis did not indicate drug instability in the beads during preparation or when they were stored at an accelerated temperature. *In vivo* experiments on male Wistar rats revealed controlled hypoglycemic activity to a significant level for up to 10 h. Thus, we concluded that the IPNs of ALG with CMLBG could replace Ca^{2+} -ALG beads in terms of prolonged drug release and could be useful for the control of diabetes.

REFERENCES

- Peppas, N. A.; Khare, A. R. *Adv. Drug Delivery Rev.* **1993**, *11*, 1.
- Satish, C. S.; Satish, K. P.; Shivakumar, H. G. *Indian J. Pharm. Sci.* **2006**, *68*, 133.
- Athawale, V. D.; Kolekar, S. L.; Raut, S. S. *Polym. Rev.* **2003**, *43*, 1.
- Soppimath, K. S.; Kulkarni, A. R.; Aminabhavi, T. M. *J. Biomater. Sci. Polym. Ed.* **2000**, *11*, 27.
- Kulkarni, A. R.; Soppimath, K. S.; Aminabhavi, T. M.; Dave, A. M.; Mehta, M. H. J. *Controlled Release* **2000**, *63*, 97.
- Kulkarni, R. V.; Sa, B. *Drug Dev. Ind. Pharm.* **2008**, *34*, 1406.
- Kumbar, S. G.; Soppimath, K. S.; Aminabhavi, T. M. *J. Appl. Polym. Sci.* **2003**, *87*, 1525.
- Ray, S.; Banerjee, S.; Maiti, S.; Laha, B.; Barik, S.; Sa, B.; Bhattacharyya, U. K. *Drug Delivery* **2010**, *17*, 508.
- Rokhade, A. P.; Agnihotri, S. A.; Patil, S. A.; Mallikarjuna, N. N.; Kulkarni, P. V.; Aminabhavi, T. M. *Carbohydr. Polym.* **2006**, *65*, 243.
- Rokhade, A. P.; Shelke, N. B.; Patil, S. A.; Aminabhavi, T. M. *Carbohydr. Polym.* **2007**, *69*, 678.
- Hoffman, A. S. *Adv. Drug Delivery Rev.* **2002**, *43*, 3.
- Suthar, B.; Xiao, H. X.; Klempner, D.; Frisch, K. C. *Polym. Adv. Technol.* **1996**, *7*, 221.
- Kulkarni, A. R.; Soppimath, K. S.; Aminabhavi, T. M.; Rudzinski, W. E. *Eur. J. Pharm. Biopharm.* **2001**, *51*, 127.
- Myung, D.; Waters, D.; Wiseman, M.; Duhamel, P.-E.; Noolandi, J.; Ta, C. N.; Frank, C. W. *Polym. Adv. Technol.* **2008**, *19*, 647.
- Zhang, J.; Peppas, N. A. *Macromolecules* **2000**, *33*, 102.
- Kulkarni, A. R.; Soppimath, K. S.; Aminabhavi, T. M.; Rudzinski, W. E. *Eur. J. Pharm. Biopharm.* **2001**, *51*, 127.
- Aslani, P.; Kennedy, R. A. J. *Controlled Release* **1996**, *42*, 75.
- Gonzalez-Rodriguez, M. L.; Holgado, M. A.; Sanchez-Lafuente, C.; Rabasco, A. M.; Fini, A. *Int. J. Pharm.* **2002**, *232*, 225.
- Halder, A.; Maiti, S.; Sa, B. *Int. J. Pharm.* **2005**, *302*, 84.
- Desai, N. P.; Sojomihardjo, A.; Yao, Z.; Ron, N.; Soosiong, P. J. *Microencapsulation* **2000**, *17*, 677.
- Dea, I. C. M.; Morrison, A. *Adv. Carbohydr. Chem. Biochem.* **1975**, *31*, 242.
- Parvathy, K. S.; Susheelamma, N. S.; Tharanathan, R. N.; Gaonkar, A. K. *Carbohydr. Polym.* **2005**, *62*, 137.
- Sharma, B. R.; Dhuldhoya, N. C.; Merchant, S. N. *Sci. Tech. Entrepreneur* **2008**, *3*, 1.
- Maiti, S.; Dey, P.; Banik, A.; Sa, B.; Ray, S.; Kaity, S. *Drug Delivery* **2010**, *17*, 288.
- Ray, R.; Maiti, S.; Mandal, S.; Chatterjee, T. K.; Sa, B. *Pharmacol. Pharm.* **2010**, *1*, 9.
- Foster, R. H.; Plosker, G. L. *Pharmacoeconomics* **2000**, *18*, 289.
- Sa, B.; Setty, C. M. *Indian Pat.* 224,992 (**2008**).
- Tripathy, T.; De, B. R. *J. Phys. Sci.* **2007**, *11*, 139.
- Korsmeyer, R. W.; Gurny, R.; Doelker, E. M.; Buri, P.; Peppas, N. A. *Int. J. Pharm.* **1983**, *15*, 25.
- Said, A. A.; Hassan, R. M. *Polym. Degrad. Stab.* **1993**, *39*, 393.
- von Klaushofer, H.; Berghofer, E.; Diesner, L. *Starch* **1976**, *28*, 298.
- Vogt, S.; Heinze, T.; Rottig, K.; Klemm, D. *Carbohydr. Res.* **1995**, *266*, 315.
- Agnihotri, S. A.; Aminabhavi, T. M. *Drug Dev. Ind. Pharm.* **2005**, *31*, 491.
- Agnihotri, S. A.; Aminabhavi, T. M. *J. Controlled Release* **2004**, *96*, 245.
- Mundargi, R. C.; Shelke, N. B.; Babu, V. R.; Patel, P.; Rangaswamy, V.; Aminabhavi, T. M. *J. Appl. Polym. Sci.* **2010**, *116*, 1832.
- Kumbar, S. G.; Dave, A. M.; Aminabhavi, T. M. *J. Appl. Polym. Sci.* **2003**, *90*, 451.
- Khan, K. A. *J. Pharm. Pharmacol.* **1975**, *28*, 48.
- Kumari, K.; Kundu, P. P. *Bull. Mater. Sci.* **2008**, *31*, 159.
- Rinaki, E.; Dokoumetzidis, A.; Macheras, P. *Pharm. Res.* **2003**, *20*, 406.
- Barzegar-Jalali, M.; Maleki, N.; Garjani, A.; Khandar, A. A.; Haji-Hosseini, M.; Jabbari, R.; Dastmalchi, S. *Drug Dev. Ind. Pharm.* **2002**, *28*, 681.
- Jamzad, S.; Fassih, R. *AAPS PharmSciTech* **2006**, *7*, E1.
- Chen, J.; Liu, M.; Chen, S. *Mater. Chem. Phys.* **2009**, *115*, 339.
- Yotsuyanagi, T.; Ohkubo, T.; Ohhashi, T.; Ikeda, K. *Chem. Pharm. Bull.* **1987**, *35*, 1555.
- Dainty, A. L.; Goulding, K. H.; Robinson, P. K.; Sinpkins, I.; Trevan, M. D. *Biotechnol. Bioeng.* **1986**, *28*, 210.
- Haug, A.; Larsen, B. *Acta. Chem. Scand.* **1963**, *17*, 1466.
- Mumper, R. J.; Hoffman, A. S.; Puolakkainen, P.; Bouchard, W. R.; Gombotz, W. R. *J. Controlled Release* **1994**, *30*, 241.
- Jianqi, F. E. I.; Zhang, Z.; Zhong, L.; Gu, L. *J. Appl. Polym. Sci.* **2002**, *85*, 2423.
- Kumbar, S. G.; Kulkarni, A. R.; Aminabhavi, T. M. *J. Microencapsulation* **2002**, *19*, 173.
- Rathna, G. V. N.; Chatterji, P. R. *J. Macromol. Sci. Pure Appl. Chem.* **2001**, *38*, 43.
- Kahn, C. R.; Shechter, Y. In *Goodman and Gilman's the Pharmacological Basis of Therapeutics*, 8th ed.; Theodore, W. R., Alan, S. N., Taylor, P., Gilman, A. G., Eds.; McGraw-Hill: New York, **1991**; p 1484.